ANTIOXIDANTS & REDOX SIGNALING
Volume 24, Number 15, 2016
Mary Ann Liebert, Inc.
DOI: 10.1089/ars.2014.6128

ORIGINAL RESEARCH COMMUNICATION

Epigenetic Upregulation of Metallothionein 2A by Diallyl Trisulfide Enhances Chemosensitivity of Human Gastric Cancer Cells to Docetaxel Through Attenuating NF-κB Activation

Yuanming Pan,[1,*] Shuye Lin,[2,3*] Rui Xing,[1,*] Min Zhu,[1] Bonan Lin,[2] Jiantao Cui,[1] Wenmei Li,[1] Jing Gao,[4] Lin Shen,[4] Yuanyuan Zhao,[5] Mingzhou Guo,[6] Ji Ming Wang,[3] Jiaqiang Huang,[2,3] and Youyong Lu[1]

Abstract

Aims: Metallothionein 2A (MT2A) and nuclear factor-kappaB (NF-κB) are both involved in carcinogenesis and cancer chemosensitivity. We previously showed decreased expression of MT2A and IκB-α in human gastric cancer (GC) associated with poor prognosis of GC patients. The present study investigated the effect of diallyl trisulfide (DATS), a garlic-derived compound, and docetaxel (DOC) on regulation of MT2A in relation to NF-κB in GC cells. ***Results:*** DATS attenuated NF-κB signaling in GC cells, resulting in G2/M cell cycle arrest and apoptosis, culminating in the inhibition of cell proliferation and tumorigenesis in nude mice. The anti-GC effect of DATS was attributable to its capacity to epigenetically upregulate MT2A, which in turn enhanced transcription of IκB-α to suppress NF-κB activation in GC cells. The combination of DATS with DOC exhibited a synergistic anti-GC activity accompanied by MT2A upregulation and NF-κB inactivation. Histopathologic analysis of GC specimens from patients showed a significant increase in MT2A expression following DOC treatment. GC patients with high MT2A expression in tumor specimens showed significantly improved response to chemotherapy and prolonged survival compared with those with low MT2A expression in tumors. ***Innovation and Conclusion:*** We conclude that DATS exerts its anti-GC activity and enhances chemosensitivity of GC to DOC by epigenetic upregulation of MT2A to attenuate NF-κB signaling. Our findings delineate a mechanistic basis of MT2A/NF-κB signaling for DATS- and DOC-mediated anti-GC effects, suggesting that MT2A may be a chemosensitivity indicator in GC patients receiving DOC-based treatment and a promising target for more effective treatment of GC by combination of DATS and DOC. *Antioxid. Redox Signal.* 24, 839–854.

[1]Laboratory of Molecular Oncology, Key Laboratory of Carcinogenesis and Translational Research (Ministry of Education), Peking University Cancer Hospital/Institute, Beijing, P.R. China.
[2]College of Life Sciences and Bioengineering, School of Science, Beijing Jiaotong University, 3 Shangyuancun, Haidian District, Beijing, P.R. China.
[3]Laboratory of Molecular Immunoregulation, Cancer and Inflammation Program, Center for Cancer Research, National Cancer Institute, Frederick, Maryland.
[4]Key Laboratory of Carcinogenesis and Translational Research (Ministry of Education), Department of GI Oncology, Peking University School of Oncology, Peking Cancer Hospital, Beijing, P.R. China.
[5]CAS Key Laboratory for Biomedical Effects of Nanomaterials and Nanosafety, National Center for Nanoscience and Technology of China, Beijing, P.R. China.
[6]Department of Gastroenterology and Hepatology, Chinese PLA General Hospital, Beijing, P.R. China.
*These authors contributed equally to this work.

Innovation

The primary role of metallothionein 2A (MT2A) in relation to nuclear factor-kappaB (NF-κB) activation in tumorigenesis and chemoresistance differs depending on cell types and remains to be elucidated in gastric cancer (GC). Our study provides the first evidence for epigenetic upregulation of MT2A in GC by diallyl trisulfide (DATS) and uncovers the molecular mechanisms of the anti-GC activity of DATS as well as its ability to sensitize GC cells to docetaxel (DOC) through the MT2A/NF-κB pathway. Therefore, MT2A is considered as a promising prognostic marker of sensitivity to DOC-based chemotherapy in GC patients.

Introduction

Gastric cancer (GC) is one of the most common cancers with high mortality in developing countries. Chemotherapy in addition to surgical removal is an important therapeutic modality for GC (8). Although considerable effort has been directed toward the improvement of chemotherapeutic intervention, the 5-year survival rate of GC patients remains poor partly due to the development of chemoresistance (21), raising an urgent need to seek more effective treatment strategies. Recent studies have demonstrated constitutive activation of nuclear factor-kappaB (NF-κB) in GC (10, 27, 32). Hyperactivation of NF-κB contributes to tumorigenesis by regulating cell cycle progression, promoting cancer cell proliferation, preventing apoptosis, and generating chemotherapeutic resistance (10, 25, 49, 53). Blocking NF-κB activation in cancer cells has shown promising anticancer effects (7, 10, 31).

Garlic and its derivatives have been recognized as antioxidants for cancer prevention and treatment, attributable primarily to organosulfur compounds such as diallyl trisulfide (DATS) (59). Consumption of garlic is associated with reduced incidence of GC (33, 61). The inhibitory effect of DATS on tumor growth involves multiple mechanisms such as inducing reactive oxygen species (ROS) (14), arresting cell cycle, promoting apoptosis, and suppressing proliferation, as well as blocking tumor cell invasion and metastasis (4, 28, 29, 34, 57, 60). Although the molecular mechanisms for the antitumor effect of DATS are not fully understood, the pharmacotherapeutic effects of garlic on cancer have been shown in its combined treatment with chemotherapeutic agents such as docetaxel (DOC) (7, 20). Interestingly, recent studies implicate the antitumor effect of garlic alone or in combination with DOC through inactivation of NF-κB in human cancer cells, including colon, prostate, liver, stomach, lung, and leukemic cells (7, 12, 28, 52). However, the molecular targets of DATS, in particular its effects on NF-κB in tumor cells, remain to be elucidated.

Metallothioneins (MTs) are low-molecular-weight, heavy metal-binding proteins. Human MTs consist of four isoforms, MT1, MT2A (or MT2), MT3, and MT4. In contrast to MT3 and MT4 with tissue-specific expression, MT1 and MT2A are the main MT isoforms that are well conserved and present almost in all types of soft tissues. Expression of MTs is inducible by a number of mediators and is regulated in response to exogenous signals in a cell/tissue-specific manner. Human MT genes are highly homologous and clustered in the q13 region of chromosome 16 (16q13), containing a set of MT1 genes (MT1A, B, E, F, G, H, and X genes) and one gene for each of the other MT isoforms (MT2A, MT3, and MT4) (6). MTs serve as nonenzymatic antioxidants and detoxicants involved in diverse intracellular functions, such as metal ion homeostasis, cell differentiation, apoptosis, inflammation, carcinogenesis, and chemosensitization. Aberrant expression of MTs may change their functional properties in association with tumors and neurodegeneration (46, 48).

The effects of MTs on pathophysiological processes, particularly on cancer development, are subjects of many studies. However, an intricate complexity of MT expression has been shown to associate with oncogenesis, tumor progression, and patient prognosis in different types of cancers. For instance, MT expression was augmented in breast, renal, bladder, and ovarian cancers (46, 56, 58), whereas MT expression was low due to epigenetic silencing and functioned as a tumor suppressor in a range of other human tumors, such as thyroid, esophageal, liver, colon, and prostate cancers (5, 13, 22, 38, 47, 55). In human GC, the role of MTs during tumorigenesis has been inconclusive because of the discrepancy of MT expression pattern reported (16, 24, 46). Our recent studies demonstrated that decreased MT2A in GC cell lines and primary tumors correlated with reduction of IκB-α and poor prognosis of GC patients (3, 44), suggesting an oncosuppressive role of MT2A in GC linking to NF-κB. However, the mechanisms of the regulation of MT2A and its relationship to NF-κB signaling in GC remain elusive.

Since garlic and DOC have been shown to inhibit tumor cell growth through inactivation of NF-κB in several types of cancer cells (7, 12, 28, 31, 52) and NF-κB activity during tumorigenesis may be regulated by MT2A (37, 44, 45, 50), the present study aimed to investigate the role of DATS and DOC in GC cell growth in relation to the regulation of MT2A expression and NF-κB activation. In this study, we report that DATS exerts its anti-GC activity and enhances chemosensitivity of GC to DOC by epigenetic upregulation of MT2A to attenuate NF-κB signaling. Our findings delineate a mechanistic basis of MT2A/NF-κB signaling for DATS- and DOC-mediated anti-GC effects, suggesting that MT2A may be a chemosensitivity indicator in GC patients receiving DOC-based treatment and a promising target for more effective treatment of GC by combination of DATS and DOC.

Results

DATS suppressed the proliferation and tumorigenicity of human GC cells by inducing cell cycle arrest and apoptosis

We first assessed the effect of DATS on the viability and colony formation of three human GC cell lines, BGC823, SGC7901, and AGS. DATS significantly inhibited the proliferation of GC cells (Figs. 1A, 6A, and Supplementary Fig. S1A; Supplementary Data are available online at www.liebertpub.com/ars). The antiproliferative effect of DATS on GC cells was confirmed by colony formation assay, in which GC cells treated with DATS formed significantly fewer colonies than the cells treated with saline (Figs. 1B, 6B, and Supplementary Fig. S1B). We then evaluated the effect of DATS on a subcutaneous mouse xenograft model. Intraperitoneal administration of DATS significantly reduced the volume of BGC823

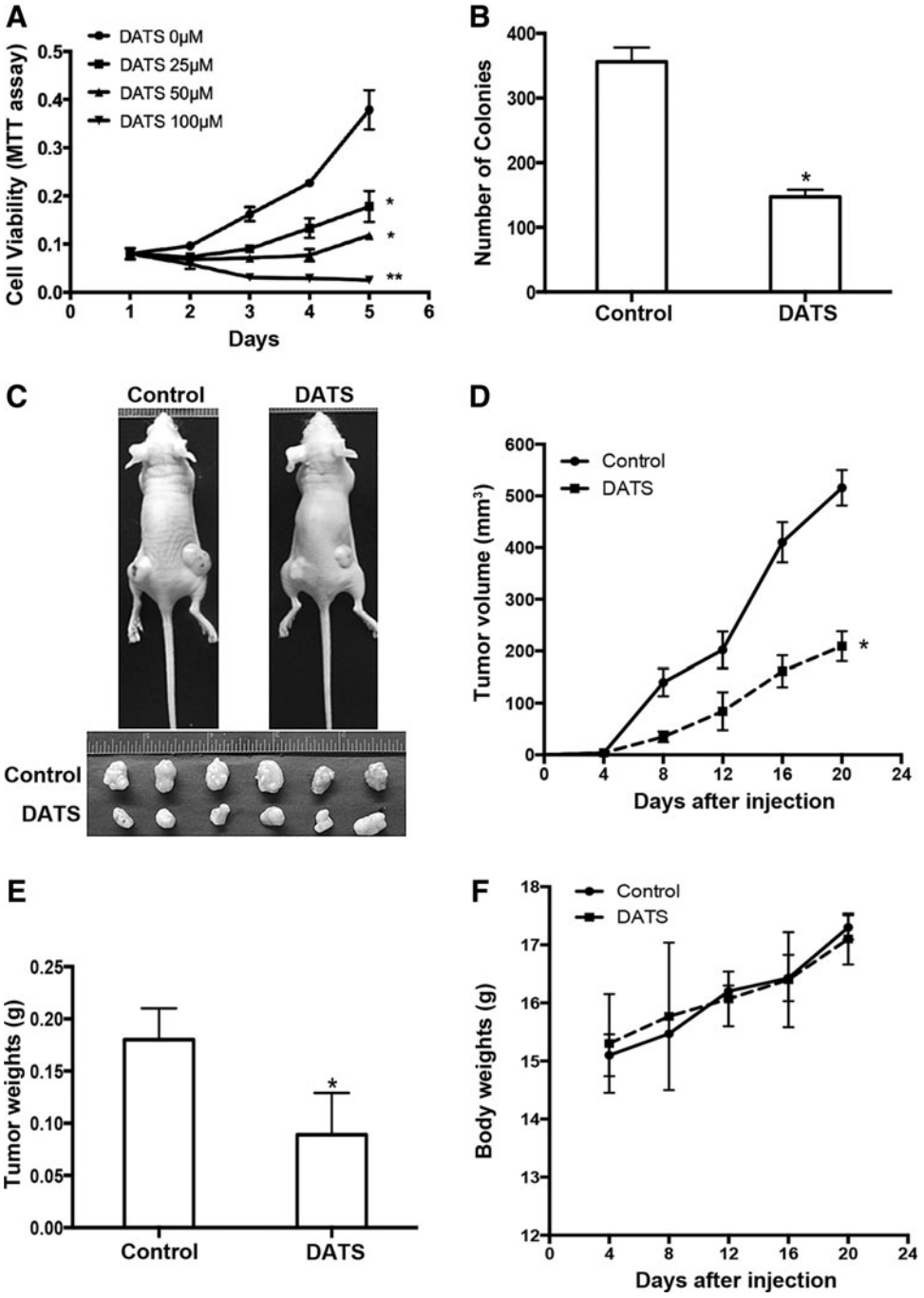

FIG. 1. The effect of DATS on the proliferation, colony formation, and tumorigenicity of human GC cells. (A) MTT assay performed to monitor the viability of BGC823 cells treated with DATS at the indicated concentrations for 4 days. Data are presented as the mean ± standard deviation ($n=3$), $*p<0.05$, $**p<0.005$, significant differences from the control. **(B)** Colony formation by GC cells in soft agar with treatment of 40 μM DATS for 4 weeks. Total number of colonies from triplicate experiments was counted. Results are shown as the mean ± standard deviation ($n=3$), $*p<0.05$ *versus* control. **(C–F)** Tumorigenicity was measured by subcutaneously injecting BGC823 cells into the left and right flanks of nude mice. After 1 day of BGC823 cell injection, the nude mice were divided into two groups and treated with 20 mg/kg of DATS or saline once every 4 days. **(C)** *Top panel*: representative image of BGC823 xenograft tumor-bearing mice treated with DATS or saline photographed at day 20. *Bottom panel*: photographs of dissected BGC823 xenograft tumors at day 20 from DATS-treated or control mice. **(D)** Tumor volume measured at the indicated times. **(E)** Tumor weight at day 20. **(F)** Body weight of tumor-bearing mice measured at the indicated times. Results shown represent the mean ± standard deviation ($n=2$ flanks ×3 mice in each group), $*p<0.05$ *versus* control. DATS, diallyl trisulfide; GC, gastric cancer.

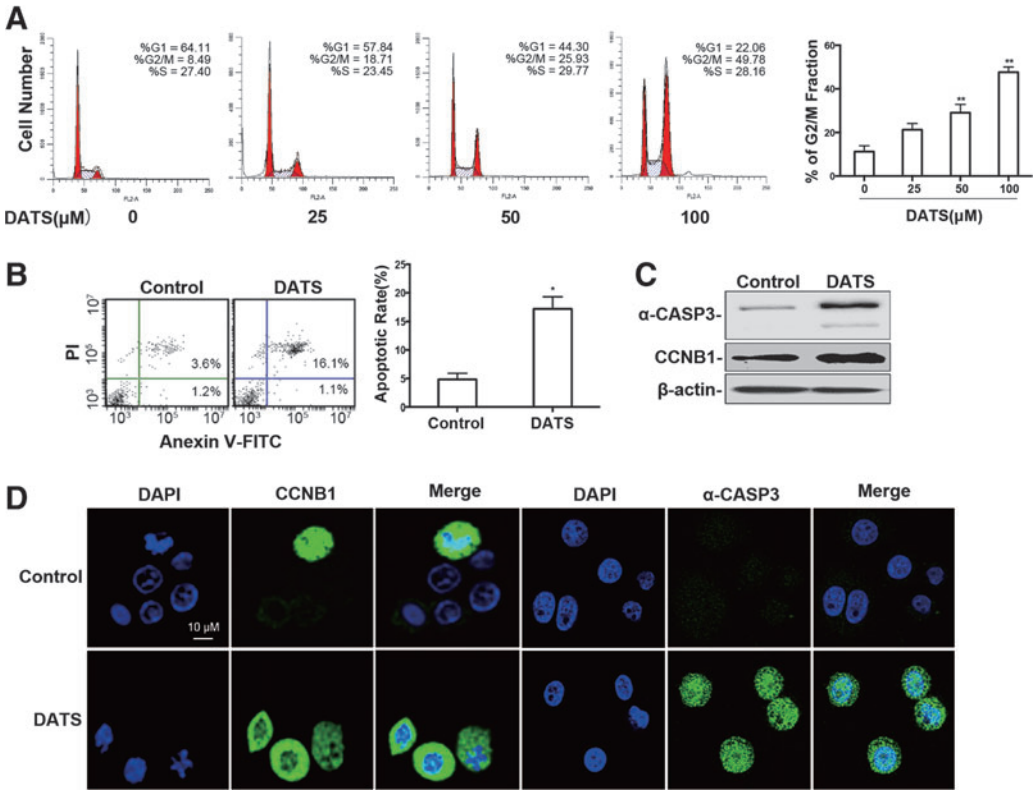

FIG. 2. The effect of DATS on cycle arrest and apoptosis of BGC823 cells. (A) FACS analysis of the cycle of BGC823 cells after 12 h of treatment with DATS at the indicated concentrations. *Left panel*: representative histograms with the percentage of cells in each cell cycle phase (*Left red peak*: G0/G1; *right red peak*: G2/M; hatched peak: S; Coefficient of variation of G1 peak: % CV). *Right panel*: quantitative analysis of G2/M phase rate from three experiments shown as the mean ± standard deviation, $^{**}p < 0.005$, DATS at indicated concentrations *versus* control. **(B)** FACS analysis of apoptosis in BGC823 cells after 12 h of treatment with DATS at 40 μM. *Left panel*: representative FACS plots. *Right panel*: quantitative data of apoptotic rate presented as the mean ± standard deviation ($n = 3$), $^{*}p < 0.05$. **(C)** Western blotting of CCNB1 and a-CASP3 protein in BGC823 cells treated with DATS (40 μM, 12 h) or saline. Results are representative of four independent experiments. **(D)** Immunofluorescence staining of CCNB1 and a-CASP3 in BGC823 cells treated with DATS (40 μM, 12 h) or saline. Nuclei shown by DAPI staining (*blue*). Shown are results from one of two comparable experiments. Scale bars, 10 μM. a-CASP3, activated caspase-3.To see this illustration in color, the reader is referred to the web version of this article at www.liebertpub.com/ars

xenograft tumors in nude mice compared with tumors formed in untreated control mice (Fig. 1C, D). DATS-treated mice also showed a marked reduction of xenograft tumor weight compared with control mice (Fig. 1E). Injection of DATS with a dose of 20 mg/kg up to 20 days did not cause weight loss in tumor-bearing mice (Fig. 1F), indicating the safety of DATS treatment. Similar results were observed in SGC7901 cell xenograft tumors in mice treated with DATS (Supplementary Fig. S2A–C). The data demonstrate the ability of DATS to suppress the tumorigenesis of human GC cells in nude mice.

We next examined cell cycle distribution and apoptosis of GC cells treated with DATS. FACS analysis demonstrated accumulation of BGC823 cells in G2/M phase at 12 h after DATS treatment (Fig. 2A). At this time point, DATS treatment caused a significant increase in the percentage of late apoptotic cells (Fig. 2B). Western blotting also showed that DATS treatment of GC cells enhanced the expression of cyclin B1 (CCNB1) and activated caspase-3 (a-CASP3), two key proteins indicating G2/M phase arrest and apoptosis of the cells (Fig. 2C, 6E, and Supplementary Fig. 4C, D). Immunofluorescence staining confirmed the expression of CCNB1 and a-CASP3 induced by DATS in GC cells (Fig. 2D). These results support our previous observation with the BGC823 cell line (34), indicating that DATS suppresses the growth of GC cells associated with G2/M phase arrest and apoptosis.

DATS attenuated NF-κB activation in GC cells

To examine the role of DATS in regulating NF-κB activation in GC cells, treatment of GC cells with DATS resulted in an increase in total IκB-α, but decrease in the NF-κB target gene cyclin D1 (CCND1) at both mRNA (Fig. 3A) and protein levels (Fig. 3B), in association with reduced phosphorylation of IκB-α (p-IκB-α) (Fig. 3B). Moreover, the expression of Bax, a proapoptotic protein, was increased in DATS-treated GC cells, whereas substantial reduction of X-linked inhibitor of apoptosis protein (XIAP) and NF-κB p65 phosphorylation (p-P65) was observed upon DATS treatment (Fig. 6E). Because both increased IκB-α expression and reduced p-IκB-α contribute to trapping NF-κB in the cytoplasm, we determined the distribution of NF-κB p65 subunit in BGC823 cells upon DATS treatment. Although no apparent change of total p65 subunit of NF-κB was observed in the whole cell extracts from BGC823 cells treated with DATS for 12 h (Fig. 3A, B), there was a time-dependent augmentation of p65 in the cell cytoplasm, with progressive

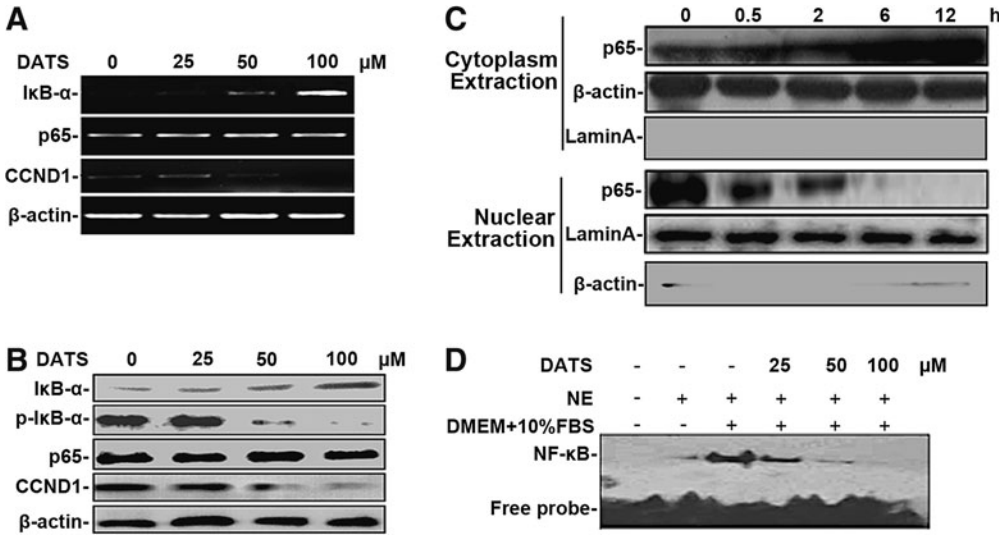

FIG. 3. The effect of DATS on NF-κB activity in GC cells. (A) RT-PCR. **(B)** Western blotting of mRNA and protein of NF-κB pathway genes in BGC823 cells after 12 h of treatment with DATS at the indicated concentrations. **(C)** Western blotting of NF-κB p65 subunit from nuclear and cytoplasmic extracts of BGC823 cells treated with 40 μM DATS at the indicated time points. β-Actin and lamin A serve as cytoplasmic and nuclear protein loading controls. **(D)** Electrophoretic mobility shift assay of DNA binding to NF-κB in the nuclei extracted from BGC823 cells after DATS treatment for 12 h at different concentrations. Results in **(A–D)** are representative from at least two independent experiments. NF-κB, nuclear factor-kappaB; RT-PCR, reverse transcription–polymerase chain reaction.

diminution in the nuclei (Fig. 3C), suggesting that DATS inhibits NF-κB activation in GC cells *via* blocking NF-κB p65 subunit translocation. The inhibitory effect of DATS on NF-κB translocation was validated by electrophoretic mobility shift assay (EMSA), in which the DNA binding capacity of NF-κB in the nuclei extracted from BGC823 cells was attenuated by DATS treatment (Fig. 3D). These results suggest that DATS treatment attenuates NF-κB activity through modifying the expression of NF-κB pathway genes in GC.

DATS induced the expression of MT2A in GC cells through an epigenetic mechanism

Based on the observation that NF-κB activity may be regulated either by DATS treatment or MT2A in GC cells (7, 10, 44), we investigated the role of MT2A in the inhibition of NF-κB and the growth of GC cells by DATS. We found that DATS dose-dependently increased the expression of MT2A at both mRNA and protein levels in GC cells (Fig. 4A, B, and Supplementary Fig. S3A, B). However, DATS did not affect the transcription of three MT1 isoforms, MT1E, MT1F, or MT1G, which show high nucleotide sequence similarity to MT2A than any other MT isoforms (44) (Fig. 4C). These findings indicate that MT2A is selectively induced by DATS in GC cells.

To elucidate the mechanisms of MT2A induction by DATS, we used a histone deacetylase (HDAC) inhibitor, trichostatin A (TSA). TSA enhanced the expression of MT2A or MT1G, but not MT1E or MT1F, in GC cells (Fig. 4C, D), suggesting that DATS-mediated MT2A induction is mimicked by TSA. Moreover, Western blotting analysis showed that DATS increased histone 3 acetylation at lysine 9 (H3K9ac) and histone 4 acetylation at lysine 5 (H4K5ac) in GC cells, accompanied with reduction of HDAC1/2 (Fig. 4E), suggesting that DATS inhibits the expression of HDACs resulting in increased histone acetylation in GC cells.

To analyze whether histone hyperacetylation mediated by DATS was associated with the MT2A gene, chromatin immunoprecipitation (ChIP) assay was performed in DATS- or TSA-treated GC cells. PCR analysis of genomic DNA immunoprecipitated by anti-H3K9ac antibody showed that H3K9ac was significantly enriched in the MT2A promoter (Fig. 4F). Thus, DATS inhibits the expression of HDACs, resulting in histone hyperacetylation of the MT2A gene in GC cells to provide accessible chromatin in favor of MT2A transcription.

DATS inhibited GC cell growth through an MT2A/NF-κB signaling pathway

In support of the capacity of DATS to inhibit GC cell growth through an MT2A/NF-κB pathway, Figure 5A shows that both DATS treatment and ectopic expression of MT2A upregulated IκB-α, but downregulated CCND1, and dephosphorylated IκB-α in BGC823 cells. The effects were further enhanced in MT2A overexpressing GC cells (MT2A-BGC823) treated with DATS. As expected, the number of apoptotic cells induced by DATS was augmented in MT2A-BGC823 cells (Fig. 5B). In contrast, transfection of BGC823 cells with MT2A mRNA-specific short hairpin RNA (shMT2A) (44) impaired DATS-mediated MT2A expression, accompanied by restoration of NF-κB activation (Fig. 5C) and a marked diminution in the percentage of apoptotic cells induced by DATS (Fig. 5D). Therefore, the effect of DATS on NF-κB inactivation and apoptosis in GC cells is attributable to its capacity to induce MT2A and IκB-α expression.

We further examined the relationship between DATS-induced MT2A expression and IκB-α activity by transfection of DNA constructs containing an IκB-α promoter region (pIκB-α-Luc, from −2 kb to transcription start site [TSS]) into BGC823 cells (Fig. 5E). As shown in Figure 5F, DATS

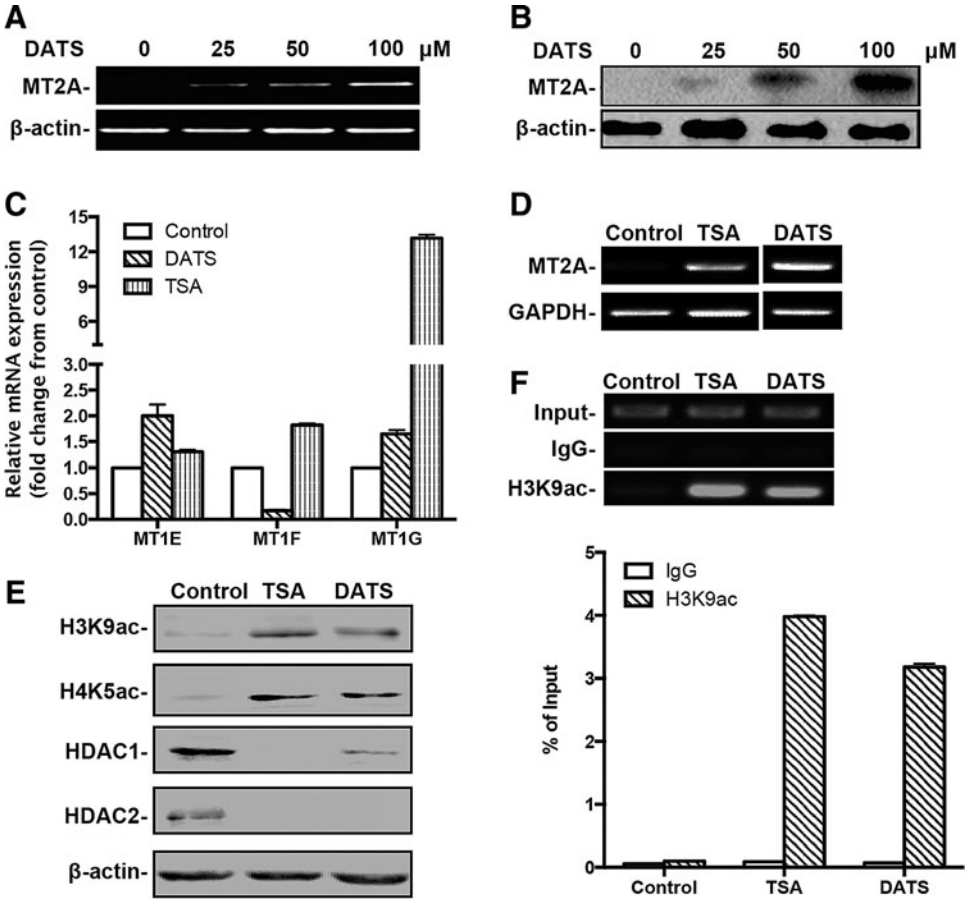

FIG. 4. Epigenetic regulation of MT2A in GC cells by DATS. **(A)** RT-RCR and **(B)** Western blotting of MT2A expression in BGC823 cells after 12 h of treatment with DATS at different concentrations. **(C)** qPCR of the expression of MT1E, MT1F, and MT1G in BGC823 cells after DATS treatment (40 μM, 12 h). The mRNA of each gene was compared with its own control after normalization against GAPDH, presented as the mean ± standard deviation. **(D)** RT-PCR and **(E)** Western blotting of BGC823 cells after DATS (40 μM, 12 h) or TSA (5 μM, 24 h) treatment. **(F)** ChIP was performed on BGC823 cells after DATS (40 μM, 12 h) or TSA (5 μM, 24 h) treatment using antibody against H3K9ac or control IgG. Precipitated ChIP DNA fractions were analyzed by PCR using primers specific for the MT2A gene (<+1 kb from TSS). *Top panel*: representative conventional PCR products visualized on 1.5% agarose gel to analyze the association of H3K9ac to the MT2A gene. *Bottom panel*: qPCR analysis of the enrichment of H3K9ac at the MT2A gene, expressed as the percentage of input. Results are representative from at least three independent experiments. ChIP, chromatin immunoprecipitation; H3K9ac, histone 3 acetylation at lysine 9; TSA, trichostatin A; TSS, transcription start site.

significantly augmented IκB-α promoter luciferase activity in GC cells, consistent with our previous result of ectopic expression of MT2A in GC cells (44). ChIP assay was performed with DATS-treated BGC823 cells by using anti-MT2A antibody to verify the association of MT2A with the promoter region of the IκB-α gene. PCR analysis of immunoprecipitated DNA fractions showed the products amplified by ChIP primer sets P4 and P5 (Fig. 5E, G, and Supplementary Table S1), but not P1 to P3 (data not shown), suggesting a physical association of MT2A protein with the proximal promoter region in the IκB-α gene from −494 to +181 of the TSS. To determine the functional consequence of MT2A enrichment in the IκB-α promoter region, luciferase plasmids, pIκB-α-4-Luc or pIκB-α-5-Luc (constructed with IκB-α promoter region from −494 to −212 or −308 to +181 of TSS, respectively), were cotransfected with plasmids pcDNA3.1-MT2A into BGC823 cells (Fig. 5E and Supplementary Table S1). Transfection of pIκB-α-4-Luc or pIκB-α-5-Luc resulted in a significant increase of IκB-α promoter luciferase activity in BGC823 cells only when cotransfected with pcDNA3.1-MT2A (Fig. 5H), supporting the previous observation that MT2A may directly target the IκB-α promoter (44). Thus, MT2A induced by DATS in GC cells is likely to suppress NF-κB activation by directly enhancing IκB-α transcription as well as inhibiting the phosphorylation of IκB-α.

To obtain *in vivo* support of the results, immunohistochemistry (IHC) analysis of tumor sections from GC xenograft tumors showed that DATS treatment increased MT2A expression associated with upregulation of IκB-α and CCNB1, but downregulation of CCND1, as well as the dephosphorylation of IκB-α (Fig. 7D and Supplementary Fig. S2D), suggesting that DATS inhibits GC cell growth *via* the MT2A/NF-κB pathway.

To demonstrate if impairing *in vivo* MT2A upregulation by DATS critically affects its antitumor activity, we performed additional *in vivo* experiments. The results showed that although the *in vivo* antitumor activity of DATS is not completely abrogated, it was significantly attenuated by shMT2A

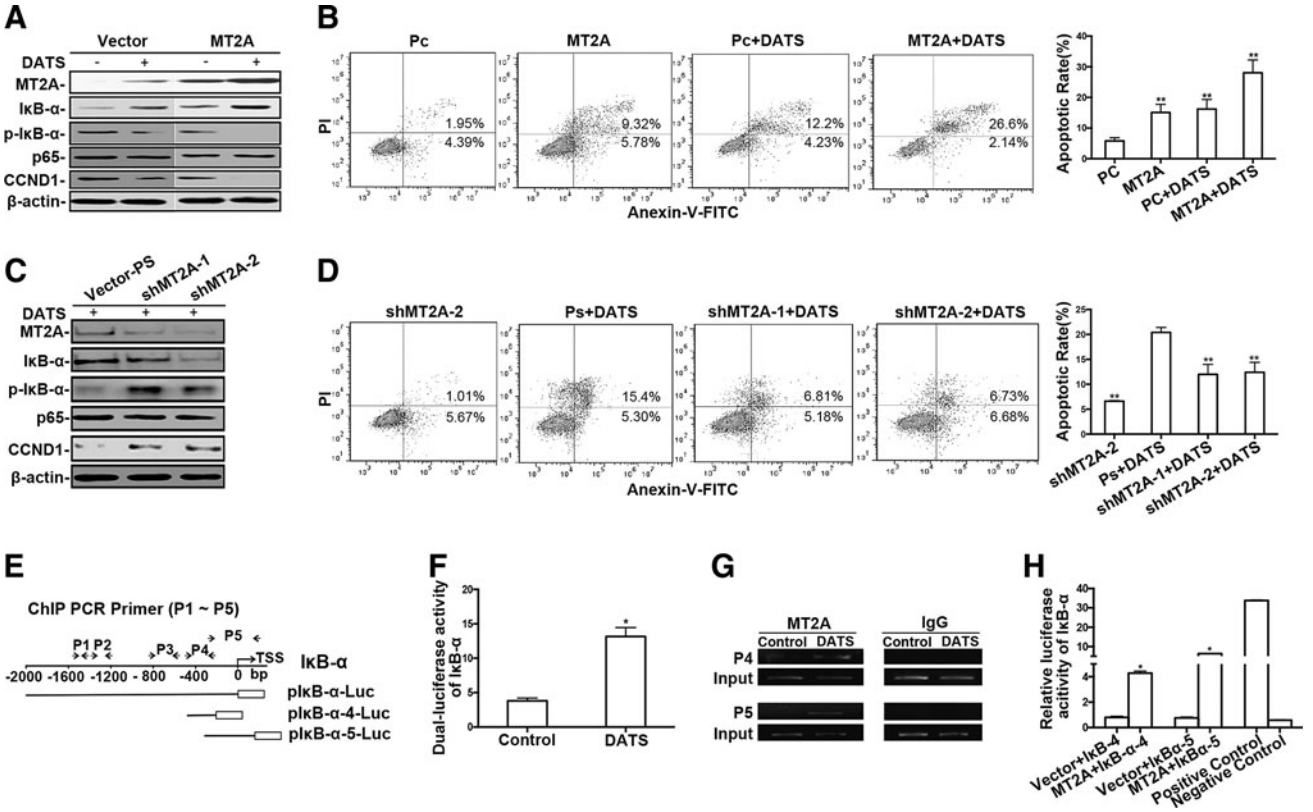

FIG. 5. The effect of DATS on the expression and function of MT2A, as well as the relationship with NF-κB in GC cells. BGC823 cells were transfected with ectopic MT2A for 36 h, followed by 40 μM DATS treatment for 12 h **(A)**, or BGC823 cells were treated with 40 μM DATS for 6 h, and recultured in fresh complete medium for transfection of shMT2A for 48 h **(C)**. Cell extracts were immunoblotted for determination of MT2A, IκB-α, p65, CCND1, and p-IκB-α. Flow cytometry of apoptosis in BGC823 cells transfected with ectopic MT2A **(B)** or shMT2A **(D)**. Cells transfected with control vector (Pc) or shMT2A-2 were used as negative controls. *Left panel*: representative results; *Right panel*: summary of apoptosis assays, presented as the mean ± standard deviation ($n = 3$), $^{**}p < 0.01$ *versus* Pc control **(B)** or Ps+DATS (D). **(E)** A schematic illustration of IκB-α promoter regions constructed into luciferase reporters: pIκB-α-Luc (–2kb/0 from TSS), pIκB-α-4-Luc (–494/–212 from TSS), and pIκB-α-5-Luc (–308/+181 from TSS), and the promoter regions covered by ChIP primers, including the primer set 4 (P4) (–494/–212 from TSS) and primer set 5 (P5) (–308/+181 from TSS). The sequences and the positions of luciferase reporter constructs and ChIP primers are shown in Supplementary Table S1. **(F)** Luciferase reporter assay showing IκB-α activities in BGC823 cells transfected with IκB-α promoter construct, pIκB-α-Luc, for 36 h, followed by 12 h of treatment with 40 μM DATS or saline. The data are presented as the mean ± standard deviation ($n = 3$), $^{*}p < 0.05$ *versus* control. **(G)** ChIP assay to identify *in vivo* association of DATS-induced MT2A with IκB-α promoter using antibody specific for MT2A, or normal IgG, followed by PCR amplification with primers specific for different IκB-α promoter regions (P1 to P5). Chromatin (1% of input) was used as input control. PCR products were visualized on a 1.5% agarose gel. PCR products amplified by ChIP primer sets 4 and 5 are shown. **(H)** Luciferase assay measuring IκB-α activities in BGC823 cells transiently cotransfected with pIκB-α-4-Luc or pIκB-α-5-Luc. pcDNA3.1-MT2A and pRL-TK serve as internal controls. pGL-3-control vector and pGL-3-basic vector serve as positive and negative controls. The experiments were repeated at least thrice, and the results are presented as the mean ± standard deviation, $^{*}p < 0.05$, *versus* control. CCND1, cyclin D1.

injection (Supplementary Fig. S6A–C). The Supplementary Figure S6D shows that MT2A upregulated by DATS in GC cells was efficiently silenced by using shMT2A in association with restoration of p-IκB-α, but reduction in IκB-α. These results, in support of our other *in vitro* and *in vivo* data, confirm the anti-GC activity of DATS *via* an MT2A/NF-κB signaling pathway in both *in vitro* and *in vivo* experiments.

DATS in combination with DOC showed enhanced anti-GC activity

Since DOC in combination with garlic or other compounds has been shown to synergistically induce mitotic catastrophe and apoptosis in many cancer cells (7, 14, 20, 31), we evaluated the effect of a combination regimen of DATS and DOC on the growth of GC. Treatment of GC cells with a combination of DATS and DOC (DATS+DOC) resulted in synergistic inhibition on cell growth, as demonstrated by reduced cell viability (Fig. 6A) and colony formation (Fig. 6B). Treatment of BGC823, SGC7901, and AGS cells with DATS or DOC alone increased cell arrest in the G2/M phase, which was synergistically enhanced by the combination of two agents (Fig. 6C and Supplementary Fig. S4A). FACS analysis showed that DATS+DOC increased the number of GC cells in late apoptosis compared with either DATS or DOC alone (Fig. 6D and Supplementary Fig. S4B). Western blotting

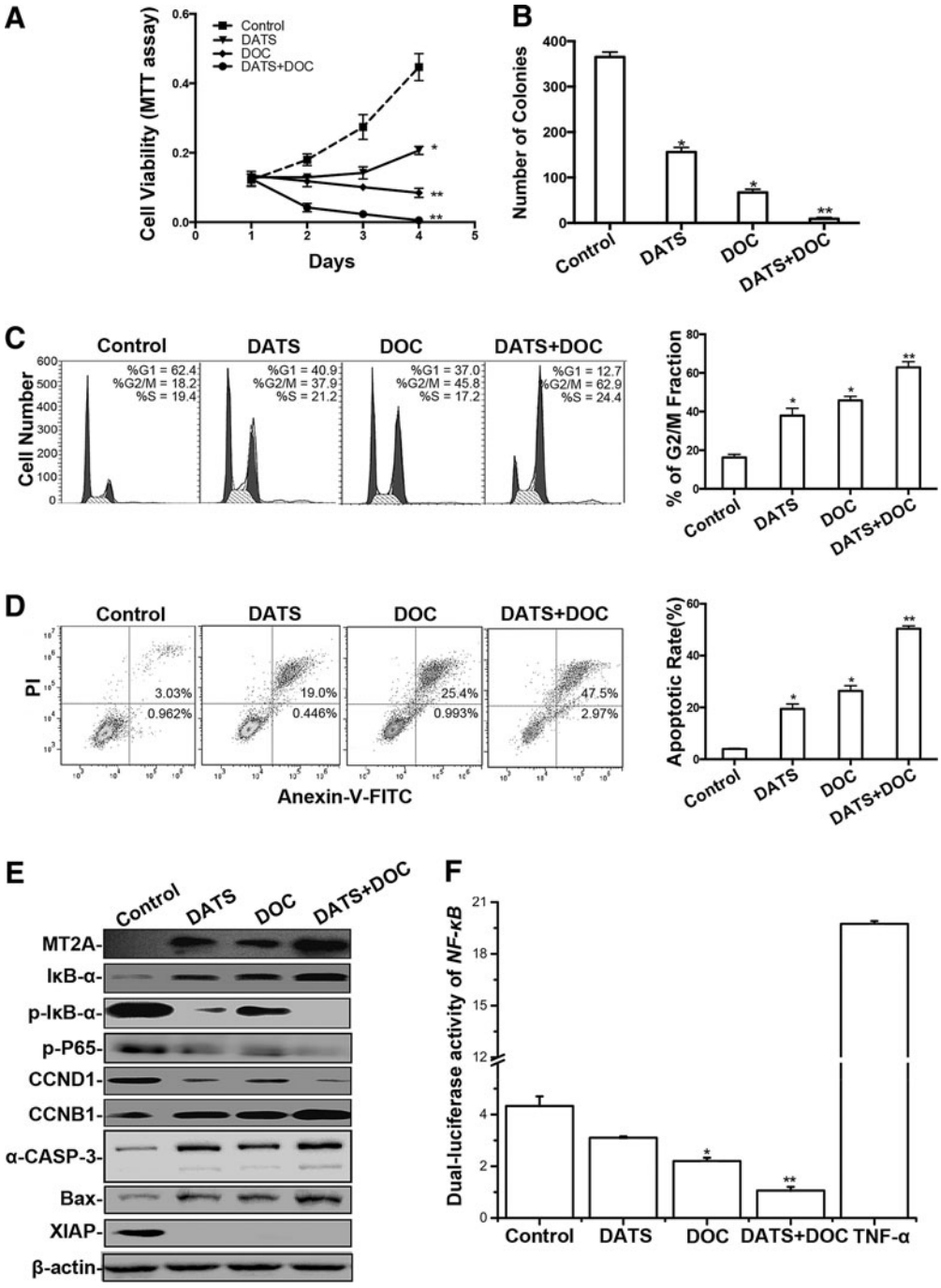

FIG. 6. The anti-GC activity of DATS in combination with DOC in relation to MT2A expression and NF-κB activation. **(A)** MTT assay monitoring the viability of BGC823 cells treated with 40 μM DATS, 10 nM DOC, and the combination (40 μM DATS +10 nM DOC) for 3 days. **(B)** Colony formation by BGC823 cells treated with DATS (40 μM) and/or DOC (10 nM) once a week for 4 weeks. *Left panel*: representative analysis of cell cycle distribution **(C)** and apoptosis **(D)** of BGC823 cells after treatment with DATS and/or DOC. *Right panel*: quantitation. **(E)** Western blotting of BGC823 cells upon indicated treatment. **(F)** Luciferase assay measuring NF-κB activity in BGC823 cells. BGC823 cells were transiently cotransfected with pNF-κB-Luc and pRL-TK, with or without pcDNA3.1-MT2A, for 24 h, and then were treated with DATS (40 μM) and/or DOC (10 nM) for another 12 h. Cells incubated with TNF-α serve as positive control. Relative luciferase activities were relative to luciferase activity in unstimulated cells. Data from at least three independent experiments are presented as the mean ± standard deviation, $*p < 0.05$, $**p < 0.01$ *versus* control. DOC, docetaxel; TNF-α, tumor necrosis factor-alpha.

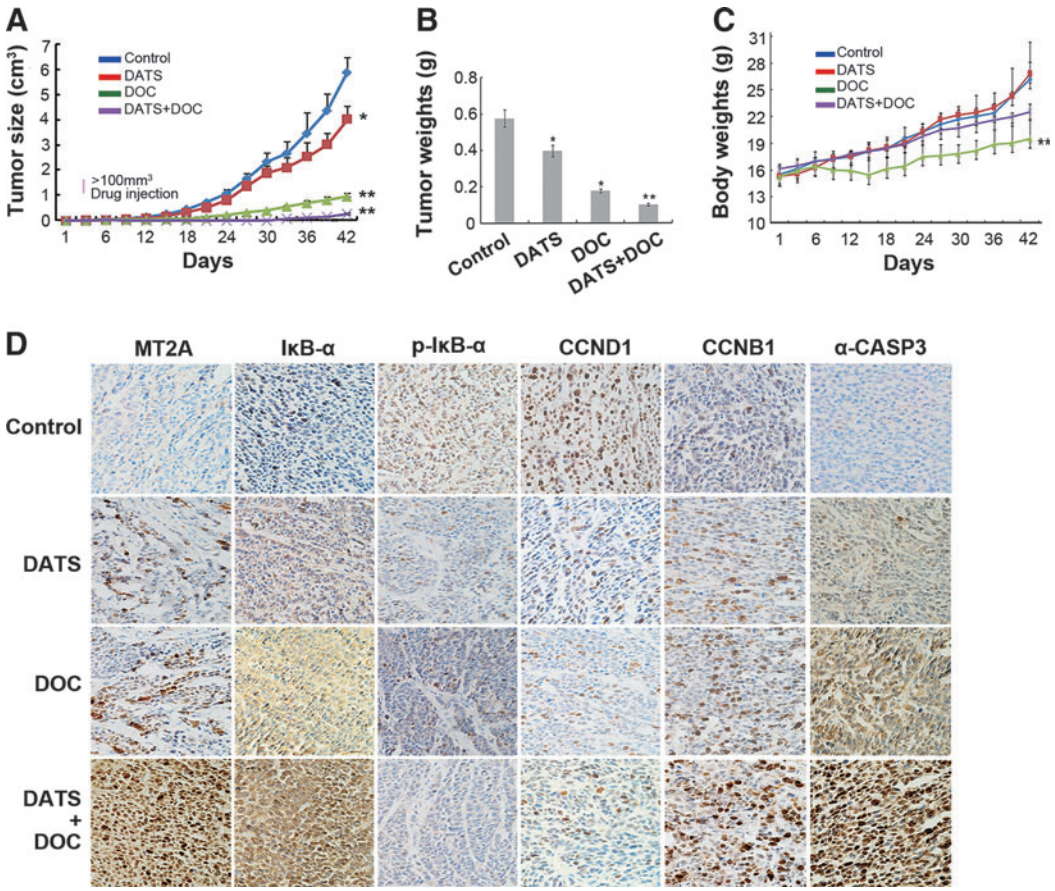

FIG. 7. The effect of DATS combined with DOC on the growth of BGC823 xenograft tumors. Tumorigenicity was examined by subcutaneous injection of BGC823 into nude mice. The mice with tumor xenografts of ~100 mm^3 in size at day 6 were treated with DATS (i.p., 20 mg/kg) and/or DOC (i.p., 10 mg/kg) twice per week. Tumor volume of BGC823 xenograft and body weight of the mice were measured every 3 days until the animals were sacrificed at day 42. **(A)** Tumor volume measured at the indicated times, **(B)** weight of the xenograft tumors isolated at day 42. **(C)** Body weight of tumor-bearing mice measured at the indicated times. Results shown represent the mean ± standard deviation, $n = 2$ flanks ×3 mice in each group, $*p < 0.05$, $**p < 0.01$, significant differences from the control. **(D)** Immunohistochemical staining of isolated BGC823 xenograft tumors. Brown staining indicates the expression of MT2A, IκB-α, p-IκB-α, CCND1, CCNB1, or a-CASP3, respectively. Magnifications: ×200. i.p., intraperitoneal injection. To see this illustration in color, the reader is referred to the web version of this article at www.liebertpub.com/ars

confirmed increased MT2A, IκB-α, CCNB1, a-CASP3, and Bax, but decreased p-IκB-α, p-P65, CCND1, and XIAP, expression upon treatment of GC cells with DATS+DOC compared with either agent alone (Fig. 6E and Supplementary Fig. S4C, D). These results indicate that the anti-GC effect of DOC is associated with its capability to induce MT2A expression and suppress NF-κB activation, which is further enhanced in combination with DATS. Moreover, luciferase assays showed that combined treatment with DATS and DOC resulted in synergistic inhibition on the transcriptional activity of NF-κB in GC cells (Fig. 6F). Thus, DATS in combination with DOC exerts a synergistic anti-GC effect through the regulation of the MT2A/NF-κB pathway.

To further investigate the effect of DATS in combination with DOC on BGC823 xenograft tumor growth in nude mice, Figure 7A, B, and Supplementary Figure S5 show that treatment with DATS or DOC alone for 42 days significantly inhibited tumor growth *in vivo*, with enhanced effect seen in combined treatment with DATS and DOC. Tumor-bearing mice in all groups did not show moribund conditions. However, in contrast to reduced body weight of tumor-bearing mice treated with DOC alone, mice treated with DATS showed a comparable weight to control mice, and interestingly, DATS+DOC treatment significantly reduced weight loss of mice compared with DOC treatment alone (Fig. 7C). These results indicate that DATS+DOC possessed enhanced anti-GC activity with fewer side effects in mice. IHC analysis of tumor sections from BGC823 xenograft tumors showed higher expression of MT2A after DATS+DOC treatment compared with either agent alone. This was associated with upregulation of IκB-α, CCNB1, and a-CASP3, but downregulation of CCND1, as well as dephosphorylation of IκB-α (Fig. 7D). Thus, the combination of two agents demonstrates an enhanced effect of anti-GC activity in which DATS-induced MT2A may promote the sensitivity of GC to DOC.

Upregulation of MT2A in tumors of GC patients upon DOC treatment was associated with increased chemotherapeutic efficiency and prolonged survival

To explore whether MT2A expression in tumors is correlated with clinical outcome of GC patients who received

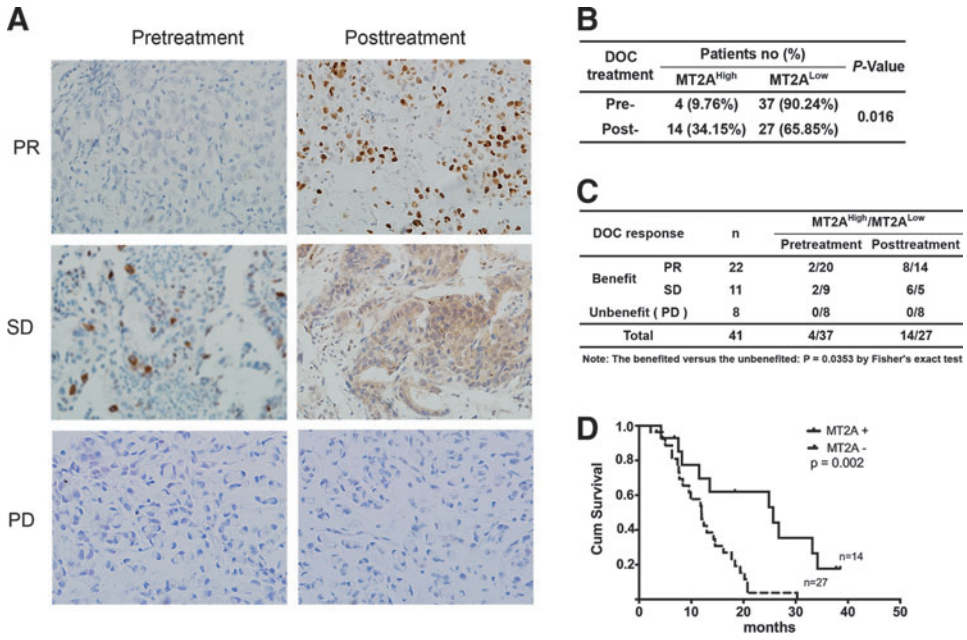

FIG. 8. The association between MT2A expression and the clinical outcome of GC patients receiving DOC treatment. (A) Representative immunohistochemical staining; magnifications: ×200. **(B)** Analysis of the status of MT2A expression in 41 paired GC specimens from patients before and after DOC treatment ($p=0.01$ by Fisher's test). **(C)** Analysis of the association between the therapeutic efficacy of DOC and MT2A expression in the tumor of GC patients. Patients benefited *versus* unbenefited: $p=0.0353$ by Fisher's exact test. **(D)** Kaplan–Meier analysis of survival of GC patients with MT2A expression in the tumors upon DOC treatment. $MT2A^{High}$, high expression of MT2A in tumor tissues; $MT2A^{Low}$, low expression of MT2A in tumor tissues; PD, progressive disease; PR, partial response; SD, stable disease. To see this illustration in color, the reader is referred to the web version of this article at www.liebertpub.com/ars

DOC treatment, we investigated MT2A expression in tumor tissues collected from GC patients before and after DOC treatment. Among 41 GC patients receiving DOC treatment, 33 (80.49%) were classified as clinically beneficial responders or effective responders based on a partial response (PR) (6) or stable disease (SD), whereas 8 (19.51%) patients with progressive disease (PD) were considered as ineffective responders ($p=0.0353$ as evaluated by Fisher's exact test) (Fig. 8C, Table 1, and Supplementary Table S2). The number of patients with high expression of MT2A in tumor tissues ($MT2A^{High}$) was significantly increased upon DOC treatment (Expression rate: pretreatment 9.76% *vs.* post-treatment 34.15%; $p=0.016$, Fig. 8B). As shown in Figure 8A, IHC demonstrated clearly increased expression of MT2A in tumors from patients with PR and SD after DOC treatment compared with low MT2A expression in tumor tissues

TABLE 1. THE RELATIONSHIP BETWEEN MT2A EXPRESSION AND CLINICOPATHOLOGICAL FEATURES OF GASTRIC CANCER PATIENTS TREATED WITH DOCETAXEL

Clinical feature	*Patient nos. (%)* (n = *41*)	*MT2A*^{High}	*MT2A*^{Low}	*Ratio*	p-*Value*
Gender					
Male	32 (78.05%)	10 (31.25%)	22 (68.75%)		
Female	9 (21.95%)	4 (44.44%)	5 (55.56%)	–0.115	0.360
Age (years)					
≥60	21 (51.22%)	6 (28.57%)	15 (71.43%)		
<60	20 (48.78%)	8 (40.00%)	12 (60.00%)	–0.120	0.329
Tumor differentiation					
Moderate	7 (17.07%)	5 (71.43%)	2 (28.57%)		
Moderate-poor	18 (43.90%)	8 (44.44%)	10 (55.56)		
Poor	16 (39.03%)	1 (6.25%)	15 (93.75%)	–0.351	0.024
GC type					
Intestinal	34 (82.90%)	13 (38.24%)	21 (61.76%)		
Diffuse	7 (17.10%)	1 (14.29%)	6 (85.71%)	0.190	0.224
Clinical benefit rate					
Yes (PR+SD)	33 (80.49%)	14 (42.42%)	19 (57.58%)		
No (PD)	8 (19.51%)	0 (0.00%)	8 (100.00%)	–0.355	0.023

GC, gastric cancer; PD, progressive disease; PR, partial response; SD, stable disease.

($MT2A^{Low}$) from PD patients. There was a fourfold increase in the number of the patients with $MT2A^{High}$ in PR and a threefold increase in SD, in contrast to no MT2A changes in tumors of PD patients (PR, SD *vs.* PD: $p = 0.0478$ assessed by Cochran–Mantel–Haenszel test, Fig. 8C). All patients with $MT2A^{High}$ after DOC treatment showed effective response (PR+SD) and better tumor differentiation compared with PD patients (Table 1). However, there was no correlation with other parameters. Among 41 GC patients with follow-up, Kaplan–Meier survival analysis showed a significantly increased survival time in $MT2A^{High}$ patients upon DOC treatment ($p = 0.002$), with a median survival time of 700 days (95% confidence interval [CI]: 194–1346 days) compared with 359 days (95% CI: 257–452 days) of $MT2A^{Low}$ patients (Fig. 8D). These results demonstrate a more favorable clinical outcome for $MT2A^{High}$ GC patients upon DOC treatment. Moreover, multivariate analysis showed that $MT2A^{High}$ was an independent factor for clinical outcome prediction ($p = 0.002$, 95% CIs: 0.074–0.557, Table 2). Thus, increased MT2A expression in GC upon DOC treatment is correlated with the therapeutic efficiency of DOC and longer survival time of GC patients. Our results indicate that $MT2A^{High}$ in GC after treatment serves as an indicator of sensitivity to DOC-based chemotherapy.

Discussion

MT genes contain multiple regulatory elements such as metal responsive element (MRE) and CCAAT/enhancer-binding protein α (C/EBPα) in their promoter regions and are transcriptionally inducible by a diverse range of factors such as metals, stress, ROS, nitrogen reactive species (NRS), hormones, proinflammatory cytokines, toxic compounds, and chemotherapeutic agents (1, 15, 23, 35, 45, 46, 48). Epigenetic silencing of MT genes was detected in several types of tumors, and epigenetic disruption of MT2A may occur in GC (15, 17, 22, 23, 38, 47). In the present study, we found that DATS, a garlic-derived antioxidant compound, significantly induced the expression of MT2A, but not other MT isoforms such as MT1E, MT1F, or MT1G in human GC cells. IHC results also demonstrated that DATS was capable of inducing the expression of MT2A in human GC cell xenograft tumors in nude mice where MT2A was silenced in tumors in non-DATS treatment mice. Despite the fact that tumor xenografts in mice often form a hypoxic and chronic inflammatory microenvironment (2), which may cause the enrichment of potential MT2A inducers, our results suggest that MT2A may not be directly affected in the tumor microenvironment, but rather tends to be selectively mediated by DATS. It was reported that there is alteration of histone modifications in MT promoter regions, which is involved in location-specific epigenetic regulation of MTs (26, 36, 47). Recent studies revealed that the anticancer activity of garlic involves inhibition of HDAC (18, 42). Consistent with these reports, we provided evidence that the suppressive effect of DATS on HDAC activity resulted in histone hyperacetylation in the MT2A promoter region in favor of MT2A transcription. The epigenetic regulation of MT2A in GC cells by DATS indicates that MT2A expression is regulated in a differential and tissue-specific manner during cancer development (6, 46).

Table 2. Multivariate COX Regression Analysis of Clinical Features Potentially Correlated with Survival of Gastric Cancer Patients

Variable factor	*Wald*	p-*Value*	*Exp (B)*	*95% CI*
$MT2A^{High}$	9.607	0.002	0.203	0.074–0.557
Clinical benefit rate	0.238	0.626	1.273	0.483–3.354
GC type (intestinal)	1.322	0.25	1.853	0.648–5.305
Age (≥60)	1.975	0.16	0.602	0.297–1.221
Sex (male)	1.803	0.179	2.146	0.704–6.539
Differentiation (moderate)	0.066	0.798	0.857	0.263–2.79

Aberrant expression of MTs may dampen their antioxidant functions resulting in tumorigenesis and chemoresistance, in which NF-κB plays a central role in the regulation of cellular survival and death (6, 46, 48). Garlic and garlic extracts as antioxidants have been reported to protect against free radical damage in tissues (59). The anticancer pharmacotherapeutic roles of DATS may be attributable to its ability to inhibit cancer cell proliferation, induce apoptosis, and perturb cell cycle in association with inhibition of NF-κB signaling, which in turn results in enhanced chemosensitivity (7, 10, 12, 28). Despite the ambiguous association between MT2A and NF-κB in the regulation of apoptosis in some tumor types, substantial evidence from MT1 and 2 double knockout (MTKO) cell lines or mice indicated that MT2A is important for inactivation of NF-κB. For instance, deficiency in MT facilitated NF-κB activation induced by TNF-α in embryonic cells (50), stimulated by mitogens in splenocytes (11), or in *Helicobacter pylori*-infected gastric cells (40) is associated with carcinogenesis (39, 41). Moreover, MTKO mice displayed increased incidence of hepatocellular carcinoma (HCC) upon diethylnitrosamine treatment accompanied by accumulation of superoxide anions and NF-κB activation in the liver (37). A recent study also demonstrated that downregulation of metallothionein 1M (MT1M) due to epigenetic silencing in human HCC may promote tumorigenesis by increasing NF-κB activity (38). In agreement with these, we showed that MT2A contributes to DATS-mediated apoptosis in GC associated with upregulation of proapoptotic proteins, such as a-CASP3 and Bax, and downregulation of antiapoptotic protein XIAP in GC cells. Moreover, we demonstrated that MT2A, either by overexpression or DATS induction, is capable of enhancing IκB-α transcription and abrogating the phosphorylation of IκB-α in GC cells. We further identified MT2A as a transcriptional cofactor associated with the proximal promoter of the IκB-α gene. Our results thus revealed that MT2A mediates the anti-GC activity of DATS *via* upregulation of IκB-α to inhibit NF-κB activation.

Since both MT2A and NF-κB are involved in the chemosensitivity of tumor cells, regulation of MT2A/NF-κB signaling may benefit the sensitivity of GC cells to chemotherapy. DOC is one of the most widely used chemotherapeutic agents, acting on several signaling pathways, including NF-κB inactivation to induce cancer cell death (14, 31). A recent report showed that S-allylmercaptocysteine derived from garlic promotes DOC-mediated prostate cancer cell death by inducing G2/M cell cycle arrest and apoptosis (20). Similarly, thiacremonone, another garlic-derived compound, augments DOC-mediated inhibition of human colon cancer cells with inactivation of NF-κB (7). Therefore, garlic in combination with DOC may synergistically induce cell

cycle arrest and apoptosis by suppressing NF-κB activation. In addition, the antioxidant effect of garlic may turn down NF-κB activity resulting in increased chemosensitivity of cancer cells to DOC. Our study showed that the combination of DATS with DOC synergistically inhibited GC cell growth by inducting G2/M cell arrest and apoptosis, accompanied by induction of MT2A and inactivation of NF-κB. More importantly, DATS treatment had no side effects and appeared to reduce the toxicity of DOC in tumor-bearing animals. In fact, DATS has been recognized as a safe agent in the suppression of tumor growth in animal models and in human epidemiological studies (7, 14, 20, 31, 33, 59, 61). It is also noteworthy that the effect of DATS and DOC on tumor growth may involve multiple mechanisms (7, 20, 59). Our results suggest that DATS-regulated MT2A/NF-κB signaling may play an important role in enhancing the chemosensitivity of GC cells to DOC.

A recent report showed that ectopic overexpression of MT1E increased the sensitivity of melanoma to cisplatin-induced apoptosis, where the MT1E gene was originally silenced due to hypermethylation in its promoter region (15). Our study thus suggests that MT2A may also act as a prognostic indicator of the chemosensitivity to DOC-based treatment of GC. However, in human breast cancer and lung cancer, overexpression of MT was reported to be associated with poor patient outcome and may favor the resistance of tumors to chemotherapeutic agents (30, 51, 56, 58). These discrepancies indicate that the regulation and function of MTs in cancer may differ in various tumor types reflecting the heterogeneity of cancer development and the requirement for personalized therapeutic strategy (44, 46, 48).

The cause for downregulation of MT2A in GC remains to be elucidated, despite a well-understood interaction between MT and oxidants in tumorigenesis (1, 54). In human HCC, PI3K/AKT inhibits the capacity of glycogen synthase kinase 3 (GSK-3) to mediate the phosphorylation of C/EBPα to initiate transcriptional activation of the MT gene in cooperation with metal transcription factor-1 (MTF-1) (13). In breast cancer cells, metal-induced expression of the MT gene was regulated by p53-induced MTF-1 to target MRE in MT promoter associated with inhibition of HDAC (43). Consistent with epigenetic regulation of MT during tumorigenesis, we recently reported that miR-23a may play a role in downregulating MT2A and promoting the proliferation of GC cells (3).

Concluding remarks

We demonstrate that MT2A upregulated by DATS, DOC, or both agents exerts suppressive activity on human GC. MT2A expression is associated with a more favorable anticancer effect of DOC and a better GC patient outcome. We also reveal the capacity of DATS to inhibit the growth of GC cells *via* the MT2A/NF-κB pathway. Furthermore, the levels of MT2A expression may be used as a marker for tumor sensitivity to DOC-based chemotherapy in GC patients and as a therapeutic target for personalized treatment of GC.

Materials and Methods

Cell culture and treatment

GC cell lines BGC823, SGC7901, and AGS and MT2A-BGC823 (stably overexpressing MT2A) were cultured as previously described (44). Cells at 60% confluence were treated with DATS (Shanghai Hefeng Company) (34) and/or DOC (Taxotere, 20 mg; Aventis Pharma Dagenham) or saline as control treatment. DATS at fixed concentration of 40 μM was used for the treatment of GC cell line based on our previous observation that DATS (25–100 μM) dose-dependently attenuated cell growth, with an IC50 value of 33.42 μM in BGC823, 55.75 μM in SGC7901, and 40.13 μM in AGS cells (unpublished data), in agreement with the dose used in other studies (19, 57). BGC823 cells were treated with TSA at concentration of 5 μM for 24 h, then harvested.

DNA constructs and transfection

Ectopic MT2A, short hairpin RNA against MT2A (shMT2A-1 and −2), and luciferase reporter containing IκB-α promoter region (pIκB-α-Luc) were constructed and transfected into BGC823 cells for transient expression as described (3, 44). Luciferase reporter plasmids, pIκB-α-4-Luc and pIκB-α-5-Luc, were constructed by cloning the proximal promoter sequence of the IκB-α gene luciferase reporter construct into BglII/HindIII sites of the pGL3-Basic reporter plasmid (Promega). NF-κB-luciferase reporter plasmid (pNF-κB-Luc) was purchased from Beyotime, Ltd. (D2206). The internal control vector, pRL-TK, was purchased from Promega. *In vitro* transfection was performed using Lipofectamine 2000 (Invitrogen) following the manufacturer's instructions. All oligonucleotide sequences are listed in Supplementary Table S1.

Patients and specimens

This study was approved by the Institutional Ethics Review Board for human investigation at Peking University. Patients with advanced GC in stage IV previously not treated with chemotherapy were enrolled into the study with neoadjuvant chemotherapy, including DOC. Endoscopical biopsy specimens of primary GC were obtained from patients before and after treatment (DOC: two cycles, 60 mg/m^2 i.v., every 3 weeks) and stored at the Tissue Bank of Peking University Cancer Hospital according to the standard procedures of the Ethics Committee of Peking University Cancer Hospital. Informed consent was obtained from patients. Clinical responses were assessed after chemotherapy. Forty-one matched pairs of GC biopsy specimens from patients before and after neoadjuvant chemotherapy with follow-up data were collected. Patients in this study were between 19 and 77 years old, including 32 males and 9 females (Table 1 and Supplementary Table S2).

RNA isolation, reverse transcription, and polymerase chain reaction

Total RNA was isolated from cells using TRIzol Reagent (Invitrogen) and reverse transcribed according to the manufacturer's instructions. PCR was performed using primers described in Supplementary Table S1. Conventional PCR products were visualized on 1.5% agarose gel. The mRNA expression levels of MT1E, MT1F, and MT1G were analyzed using SYBR Green-based qPCR reagent (Transgen, Ltd.) on ABI7500 (Applied Biosystems) (44). The relative expression level of each MT gene was normalized against GAPDH control using the $2^{-\overline{\Delta\Delta Ct}}$ method and further compared with its own control.

Western blotting

Western blotting was performed as described previously (44). Details are provided in the Supplementary Material and Methods.

Immunofluorescence

Cells were fixed with 4% paraformaldehyde at 4°C for 10 min. After washing and preblocking, the cells were incubated at 4°C overnight with antibodies against CCNB1 (1:50) and a-CASP-3 (1:50), respectively, followed by incubation with FITC-conjugated secondary antibody (1:50; Santa Cruz) for 1 h. DAPI was used for nuclear staining (10 μg/ml in phosphate-buffered saline [PBS], Invitrogen, Life Technologies). Images were then analyzed by laser confocal microscopy (Leica Sp5 Laser Scanning Confocal Microscope; GE).

Immunohistochemistry

IHC was performed on tumor sections from GC cell xenografts in nude mice, using antibodies listed in Supplementary Material and Methods. GC patient tumor specimens were analyzed and scores described previously (44).

Luciferase assay

Luciferase reporter assay was performed using a Dual-Luciferase Reporter Assay System (Promega). Luciferase reporters were transfected into BGC823 cells cultured in 35-mm dishes with or without DATS treatment as described (3, 44). All experiments were performed at least thrice.

Electrophoretic mobility shift assay

Nuclear extracts were isolated from BGC823 cells with or without DATS treatment. Nuclear proteins (3 μg) were mixed with biotin-labeled probes containing the NF-κB consensus sequence (50 fmol) (Supplementary Table S1) and incubated at room temperature for 20 min. The protein-DNA mixtures were then separated from free probe on 6% polyacrylamide gel in a 4°C cold room for 2 h in Tris-glycine-EDTA running buffer. The gel was dried, exposed to films, and analyzed by a PhosphorImager (Storm 840; Amersham Biosciences).

Chromatin immunoprecipitation

ChIP assay was performed following an EpiTech ChIPOneDay kit protocol (Qiagen). Details are described in Supplementary Material and Methods.

Cell viability and colony formation

Cell viability and colony formation were examined as previously described (3, 44). Details are given in Supplementary Material and Methods.

Cell cycle and apoptosis

Cells were seeded into 10-cm dishes (1×10^6 cells/dish) and treated with DATS and/or DOC. The cells were fixed and stained in a solution containing propidium iodide (PI) overnight at 4°C, following the instructions of the cell cycle detection kit (Beyotime Ltd.), and then analyzed by flow cytometry (BD FACS Array™ Bioanalyzer; BD Biosciences). Apoptotic cells were stained using the Apo-Alert Annexin V kit (BD Biosciences) before analysis.

Tumorigenicity

The animal handling and all *in vivo* experimental procedures were approved by the Institutional Animal Ethics Committee of Peking University Cancer Hospital. To observe the effect of DATS on tumor growth *in vivo*, 1×10^6 GC cells in 0.1 ml PBS were subcutaneously implanted in 4-week-old Balb/c female athymic mice (Vital River Laboratories) with both flank injections of BGC823 (9) or one flank injection of SGC7901 cells. After 1 day, the mice were randomly divided into two groups, followed by intraperitoneal injection (i.p.) of DATS (20 mg/kg) or saline every 4 days. Tumor diameters and body weight in GC xenograft tumor-bearing nude mice were measured and documented every 4 days until xenograft tumor-bearing mice were sacrificed at day 20 or 24. GC tumor xenografts were isolated and weighted. Another set of experiments was performed to evaluate the effect of combination of DATS with DOC and test the long-term safety and toxicity of combined treatment. Six days after subcutaneous implantation of BGC823 cells into both flanks of nude mice, the mice with tumor xenografts of about 100 mm^3 in size were randomly divided into four groups and treated with DATS (i.p., 20 mg/kg) and/or DOC (i.p., 10 mg/kg) or saline twice per week. Tumor volumes and body weights of the mice in different groups were measured twice per week until the animals were sacrificed at day 42. Tumor volume was calculated by measuring the longest (a) and shortest (b) diameters of the tumor and calculated by the following formula: $ab^2/2$, where a is for the longest diameter and b is for the shortest diameter.

Statistical analyses

Unless otherwise specified, all experiments were performed at least thrice. Data are presented as the mean ± standard deviation. If variances were homogeneous, differences were assessed by two-way ANOVA. Two-tailed χ^2 test and Student's t-test were used to compare pretreatment characteristics of patients. Cancer-related survival was analyzed using the Kaplan–Meier method and compared using log-rank tests. Spearman's rank test and Fisher's exact test were used to analyze clinicopathological correlation. A Cox proportional hazard regression model was used with associated 95% CIs and p-values. All statistical analyses were carried out using SPSS, version 16.0. A two-tailed p-value of <0.05 was considered as statistically significant.

Acknowledgments

This work was supported by grants from the National Science Foundation of China (Grant No. 81272550), the National High-Tech Research and Development Program of China (863 Program, Grant No. 2012AA02A504), and the Open Project funded by the Key laboratory of Carcinogenesis and Translational Research, Ministry of Education (2014 Open Project-), Peking University Cancer Hospital/Institute, Beijing. J.H. and J.M.W. were also funded, in part, by Federal funds from the National Cancer Institute, National Institutes of Health, under Contract No. HHSN261200800001E and were supported, in part, by the Intramural Research Program

of the NCI, NIH. S.L. and J.H. were supported by the Intramural Research funding of Beijing Jiaotong University (S12RC00030).

Ethics Approval

This study was conducted with the approval of the Institutional Ethics Standards Committee.

Author Disclosure Statement

No competing financial interests exist.

References

1. Abbassi R, Chamkhia N, and Sakly M. Chloroform-induced oxidative stress in rat liver: implication of metallothionein. *Toxicol Ind Health* 26: 487–496, 2010.
2. Aharinejad S, Paulus P, Sioud M, Hofmann M, Zins K, Schafer R, Stanley ER, and Abraham D. Colony-stimulating factor-1 blockade by antisense oligonucleotides and small interfering RNAs suppresses growth of human mammary tumor xenografts in mice. *Cancer Res* 64: 5378–5384, 2004.
3. An J, Pan Y, Yan Z, Li W, Cui J, Yuan J, Tian L, Xing R, and Lu Y. MiR-23a in amplified 19p13.13 loci targets metallothionein 2A and promotes growth in gastric cancer cells. *J Cell Biochem* 114: 2160–2169, 2013.
4. Antosiewicz J, Herman-Antosiewicz A, Marynowski SW, and Singh SV. c-Jun NH(2)-terminal kinase signaling axis regulates diallyl trisulfide-induced generation of reactive oxygen species and cell cycle arrest in human prostate cancer cells. *Cancer Res* 66: 5379–5386, 2006.
5. Arriaga JM, Greco A, Mordoh J, and Bianchini M. Metallothionein 1G and zinc sensitize human colorectal cancer cells to chemotherapy. *Mol Cancer Ther* 13: 1369–1381, 2014.
6. Babula P, Masarik M, Adam V, Eckschlager T, Stiborova M, Trnkova L, Skutkova H, Provaznik I, Hubalek J, and Kizek R. Mammalian metallothioneins: properties and functions. *Metallomics* 4: 739–750, 2012.
7. Ban JO, Lee HS, Jeong HS, Song S, Hwang BY, Moon DC, Yoon do Y, Han SB, and Hong JT. Thiacremonone augments chemotherapeutic agent-induced growth inhibition in human colon cancer cells through inactivation of nuclear factor-{kappa}B. *Mol Cancer Res* 7: 870–879, 2009.
8. Bray F, Jemal A, Grey N, Ferlay J, and Forman D. Global cancer transitions according to the Human Development Index (2008–2030): a population-based study. *Lancet Oncol* 13: 790–801, 2012.
9. Chang E, Liu H, Unterschemmann K, Ellinghaus P, Liu S, Gekeler V, Cheng Z, Berndorff D, and Gambhir SS. 18F-FAZA PET imaging response tracks the reoxygenation of tumors in mice upon treatment with the mitochondrial complex I inhibitor BAY 87-2243. *Clin Cancer Res* 21: 335–346, 2015.
10. Cho SJ, Park JW, Kang JS, Kim WH, Juhnn YS, Lee JS, Kim YH, Ko YS, Nam SY, and Lee BL. Nuclear factor-kappaB dependency of doxorubicin sensitivity in gastric cancer cells is determined by manganese superoxide dismutase expression. *Cancer Sci* 99: 1117–1124, 2008.
11. Crowthers KC, Kline V, Giardina C, and Lynes MA. Augmented humoral immune function in metallothionein-null mice. *Toxicol Appl Pharmacol* 166: 161–172, 2000.
12. Dasgupta P and Bandyopadhyay SS. Role of di-allyl disulfide, a garlic component in NF-kappaB mediated transient G2-M phase arrest and apoptosis in human leukemic cell-lines. *Nutr Cancer* 65: 611–622, 2013.
13. Datta J, Majumder S, Kutay H, Motiwala T, Frankel W, Costa R, Cha HC, MacDougald OA, Jacob ST, and Ghoshal K. Metallothionein expression is suppressed in primary human hepatocellular carcinomas and is mediated through inactivation of CCAAT/enhancer binding protein alpha by phosphatidylinositol 3-kinase signaling cascade. *Cancer Res* 67: 2736–2746, 2007.
14. Fabbri F, Amadori D, Carloni S, Brigliadori G, Tesei A, Ulivi P, Rosetti M, Vannini I, Arienti C, Zoli W, and Silvestrini R. Mitotic catastrophe and apoptosis induced by docetaxel in hormone-refractory prostate cancer cells. *J Cell Physiol* 217: 494–501, 2008.
15. Faller WJ, Rafferty M, Hegarty S, Gremel G, Ryan D, Fraga MF, Esteller M, Dervan PA, and Gallagher WM. Metallothionein 1E is methylated in malignant melanoma and increases sensitivity to cisplatin-induced apoptosis. *Melanoma Res* 20: 392–400, 2010.
16. Galizia G, Ferraraccio F, Lieto E, Orditura M, Castellano P, Imperatore V, La Manna G, Pinto M, Ciardiello F, La Mura A, and De Vita F. p27 downregulation and metallothionein overexpression in gastric cancer patients are associated with a poor survival rate. *J Surg Oncol* 93: 241–252, 2006.
17. Ghoshal K, Datta J, Majumder S, Bai S, Dong X, Parthun M, and Jacob ST. Inhibitors of histone deacetylase and DNA methyltransferase synergistically activate the methylated metallothionein I promoter by activating the transcription factor MTF-1 and forming an open chromatin structure. *Mol Cell Biol* 22: 8302–8319, 2002.
18. Hardy TM and Tollefsbol TO. Epigenetic diet: impact on the epigenome and cancer. *Epigenomics* 3: 503–518, 2011.
19. Herman-Antosiewicz A, Stan SD, Hahm ER, Xiao D, and Singh SV. Activation of a novel ataxia-telangiectasia mutated and Rad3 related/checkpoint kinase 1-dependent prometaphase checkpoint in cancer cells by diallyl trisulfide, a promising cancer chemopreventive constituent of processed garlic. *Mol Cancer Ther* 6: 1249–1261, 2007.
20. Howard EW, Lee DT, Chiu YT, Chua CW, Wang X, and Wong YC. Evidence of a novel docetaxel sensitizer, garlic-derived S-allylmercaptocysteine, as a treatment option for hormone refractory prostate cancer. *Int J Cancer* 122: 1941–1948, 2008.
21. Huang B, Sun Z, Wang Z, Lu C, Xing C, Zhao B, and Xu H. Factors associated with peritoneal metastasis in non-serosa-invasive gastric cancer: a retrospective study of a prospectively-collected database. *BMC Cancer* 13: 57, 2013.
22. Huang Y, de la Chapelle A, and Pellegata NS. Hypermethylation, but not LOH, is associated with the low expression of MT1G and CRABP1 in papillary thyroid carcinoma. *Int J Cancer* 104: 735–744, 2003.
23. Iijima Y, Fukushima T, Bhuiyan LA, Yamada T, Kosaka F, and Sato JD. Synergistic and additive induction of metallothionein in Chang liver cells. A possible mechanism of marked induction of metallothionein by stress. *FEBS Lett* 269: 218–220, 1990.
24. Janssen AM, van Duijn W, Oostendorp-Van De Ruit MM, Kruidenier L, Bosman CB, Griffioen G, Lamers CB, van Krieken JH, van De Velde CJ, and Verspaget HW. Metallothionein in human gastrointestinal cancer. *J Pathol* 192: 293–300, 2000.

25. Karin M. Nuclear factor-kappaB in cancer development and progression. *Nature* 441: 431–436, 2006.
26. Kurita H, Ohsako S, Hashimoto S, Yoshinaga J, and Tohyama C. Prenatal zinc deficiency-dependent epigenetic alterations of mouse metallothionein-2 gene. *J Nutr Biochem* 24: 256–266, 2013.
27. Kwon HC, Kim SH, Oh SY, Lee S, Lee JH, Jang JS, Kim MC, Kim KH, Kim SJ, Kim SG, and Kim HJ. Clinicopathologic significance of expression of nuclear factor-kappaB RelA and its target gene products in gastric cancer patients. *World J Gastroenterol* 18: 4744–4750, 2012.
28. Lai KC, Hsu SC, Kuo CL, Yang JS, Ma CY, Lu HF, Tang NY, Hsia TC, Ho HC, and Chung JG. Diallyl sulfide, diallyl disulfide, and diallyl trisulfide inhibit migration and invasion in human colon cancer colo 205 cells through the inhibition of matrix metalloproteinase-2, –7, and –9 expressions. *Environ Toxicol* 28: 479–488, 2013.
29. Lee BC, Park BH, Kim SY, and Lee YJ. Role of Bim in diallyl trisulfide-induced cytotoxicity in human cancer cells. *J Cell Biochem* 112: 118–127, 2011.
30. Lee SC, Xu X, Lim YW, Iau P, Sukri N, Lim SE, Yap HL, Yeo WL, Tan P, Tan SH, McLeod H, and Goh BC. Chemotherapy-induced tumor gene expression changes in human breast cancers. *Pharmacogenet Genomics* 19: 181–192, 2009.
31. Lee SY, Cho JS, Yuk DY, Moon DC, Jung JK, Yoo HS, Lee YM, Han SB, Oh KW, and Hong JT. Obovatol enhances docetaxel-induced prostate and colon cancer cell death through inactivation of nuclear transcription factor-kappaB. *J Pharmacol Sci* 111: 124–136, 2009.
32. Levidou G, Korkolopoulou P, Nikiteas N, Tzanakis N, Thymara I, Saetta AA, Tsigris C, Rallis G, Vlasis K, and Patsouris E. Expression of nuclear factor kappaB in human gastric carcinoma: relationship with I kappaB a and prognostic significance. *Virchows Arch* 450: 519–527, 2007.
33. Li H, Li HQ, Wang Y, Xu HX, Fan WT, Wang ML, Sun PH, and Xie XY. An intervention study to prevent gastric cancer by micro-selenium and large dose of allitridum. *Chin Med J (Engl)* 117: 1155–1160, 2004.
34. Li N, Guo R, Li W, Shao J, Li S, Zhao K, Chen X, Xu N, Liu S, and Lu Y. A proteomic investigation into a human gastric cancer cell line BGC823 treated with diallyl trisulfide. *Carcinogenesis* 27: 1222–1231, 2006.
35. Liu Y, Hartley DP, and Liu J. Protection against carbon tetrachloride hepatotoxicity by oleanolic acid is not mediated through metallothionein. *Toxicol Lett* 95: 77–85, 1998.
36. Majumder S, Kutay H, Datta J, Summers D, Jacob ST, and Ghoshal K. Epigenetic regulation of metallothionein-i gene expression: differential regulation of methylated and unmethylated promoters by DNA methyltransferases and methyl CpG binding proteins. *J Cell Biochem* 97: 1300–1316, 2006.
37. Majumder S, Roy S, Kaffenberger T, Wang B, Costinean S, Frankel W, Bratasz A, Kuppusamy P, Hai T, Ghoshal K, and Jacob ST. Loss of metallothionein predisposes mice to diethylnitrosamine-induced hepatocarcinogenesis by activating NF-kappaB target genes. *Cancer Res* 70: 10265–10276, 2010.
38. Mao J, Yu H, Wang C, Sun L, Jiang W, Zhang P, Xiao Q, Han D, Saiyin H, Zhu J, Chen T, Roberts LR, Huang H, and Yu L. Metallothionein MT1M is a tumor suppressor of human hepatocellular carcinomas. *Carcinogenesis* 33: 2568–2577, 2012.
39. Mita M, Satoh M, Shimada A, Azuma S, Himeno S, and Hara S. Metallothionein deficiency exacerbates chronic inflammation associated with carcinogenesis in stomach of mice infected with *Helicobacter pylori*. *J Toxicol Sci* 37: 1261–1265, 2012.
40. Mita M, Satoh M, Shimada A, Okajima M, Azuma S, Suzuki JS, Sakabe K, Hara S, and Himeno S. Metallothionein is a crucial protective factor against *Helicobacter pylori*-induced gastric erosive lesions in a mouse model. *Am J Physiol Gastrointest Liver Physiol* 294: G877–G84, 2008.
41. Mitani T, Shirasaka D, Aoyama N, Miki I, Morita Y, Ikehara N, Matsumoto Y, Okuno T, Toyoda M, Miyachi H, Yoshida S, Chayahara N, Hori J, Tamura T, Azuma T, and Kasuga M. Role of metallothionein in *Helicobacter pylori*-positive gastric mucosa with or without early gastric cancer and the effect on its expression after eradication therapy. *J Gastroenterol Hepatol* 23: e334–e339, 2008.
42. Nian H, Delage B, Pinto JT, and Dashwood RH. Allyl mercaptan, a garlic-derived organosulfur compound, inhibits histone deacetylase and enhances Sp3 binding on the P21WAF1 promoter. *Carcinogenesis* 29: 1816–1824, 2008.
43. Ostrakhovitch EA, Olsson PE, von Hofsten J, and Cherian MG. P53 mediated regulation of metallothionein transcription in breast cancer cells. *J Cell Biochem* 102: 1571–1583, 2007.
44. Pan Y, Huang J, Xing R, Yin X, Cui J, Li W, Yu J, and Lu Y. Metallothionein 2A inhibits NF-kappaB pathway activation and predicts clinical outcome segregated with TNM stage in gastric cancer patients following radical resection. *J Transl Med* 11: 173, 2013.
45. Papouli E, Defais M, and Larminat F. Overexpression of metallothionein-II sensitizes rodent cells to apoptosis induced by DNA cross-linking agent through inhibition of NF-kappa B activation. *J Biol Chem* 277: 4764–4769, 2002.
46. Pedersen MO, Larsen A, Stoltenberg M, and Penkowa M. The role of metallothionein in oncogenesis and cancer prognosis. *Prog Histochem Cytochem* 44: 29–64, 2009.
47. Peng D, Hu TL, Jiang A, Washington MK, Moskaluk CA, Schneider-Stock R, and El-Rifai W. Location-specific epigenetic regulation of the metallothionein 3 gene in esophageal adenocarcinomas. *PLoS One* 6: e22009, 2011.
48. Ruttkay-Nedecky B, Nejdl L, Gumulec J, Zitka O, Masarik M, Eckschlager T, Stiborova M, Adam V, and Kizek R. The role of metallothionein in oxidative stress. *Int J Mol Sci* 14: 6044–6066, 2013.
49. Sakamoto K, Hikiba Y, Nakagawa H, Hayakawa Y, Yanai A, Akanuma M, Ogura K, Hirata Y, Kaestner KH, Omata M, and Maeda S. Inhibitor of kappaB kinase beta regulates gastric carcinogenesis via interleukin-1alpha expression. *Gastroenterology* 139: 226–238 e6, 2010.
50. Sakurai A, Hara S, Okano N, Kondo Y, Inoue J, and Imura N. Regulatory role of metallothionein in NF-kappaB activation. *FEBS Lett* 455: 55–58, 1999.
51. Shi G, Cai L, Jiang W, and Sui G. Effects of navelbine and docetaxel on gene expression in human lung cancer cell lines. *Cell Biochem Biophys* 61: 665–671, 2011.
52. Tang FY, Chiang EP, and Pai MH. Consumption of s-allylcysteine inhibits the growth of human non-small-cell lung carcinoma in a mouse xenograft model. *J Agric Food Chem* 58: 11156–11164, 2010.
53. Ueda M, Kokura S, Imamoto E, Naito Y, Handa O, Takagi T, Yoshida N, and Yoshikawa T. Blocking of NF-kappaB activation enhances the tumor necrosis factor alpha-induced

apoptosis of a human gastric cancer cell line. *Cancer Lett* 193: 177–182, 2003.
54. Valko M, Leibfritz D, Moncol J, Cronin MT, Mazur M, and Telser J. Free radicals and antioxidants in normal physiological functions and human disease. *Int J Biochem Cell Biol* 39: 44–84, 2007.
55. Wei H, Desouki MM, Lin S, Xiao D, Franklin RB, and Feng P. Differential expression of metallothioneins (MTs) 1, 2, and 3 in response to zinc treatment in human prostate normal and malignant cells and tissues. *Mol Cancer* 7: 7, 2008.
56. Werynska B, Pula B, Muszczynska-Bernhard B, Gomulkiewicz A, Piotrowska A, Prus R, Podhorska-Okolow M, Jankowska R, and Dziegiel P. Metallothionein 1F and 2A overexpression predicts poor outcome of non-small cell lung cancer patients. *Exp Mol Pathol* 94: 301–308, 2013.
57. Xiao D and Singh SV. Diallyl trisulfide, a constituent of processed garlic, inactivates Akt to trigger mitochondrial translocation of BAD and caspase-mediated apoptosis in human prostate cancer cells. *Carcinogenesis* 27: 533–540, 2006.
58. Yap X, Tan HY, Huang J, Lai Y, Yip GW, Tan PH, and Bay BH. Over-expression of metallothionein predicts chemoresistance in breast cancer. *J Pathol* 217: 563–570, 2009.
59. Yun HM, Ban JO, Park KR, Lee CK, Jeong HS, Han SB, and Hong JT. Potential therapeutic effects of functionally active compounds isolated from garlic. *Pharmacol Ther* 142: 183–195, 2013.
60. Zhou C, Mao XP, Guo Q, and Zeng FQ. Diallyl trisulphide-induced apoptosis in human melanoma cells involves downregulation of Bcl-2 and Bcl-xL expression and activation of caspases. *Clin Exp Dermatol* 34: e537–e543, 2009.
61. Zhou Y, Zhuang W, Hu W, Liu GJ, Wu TX, and Wu XT. Consumption of large amounts of Allium vegetables reduces risk for gastric cancer in a meta-analysis. *Gastroenterology* 141: 80–89, 2011.

Address correspondence to:
Dr. Jiaqiang Huang
College of Life Sciences & Bioengineering
School of Science
Beijing Jiaotong University
3 Shangyuancun
Haidian District
Beijing 100044
P.R. China

E-mail: jqhuang@bjtu.edu.cn

Dr. Youyong Lu
Laboratory of Molecular Oncology
Key Laboratory of Carcinogenesis and Translational Research (Ministry of Education)
Peking University Cancer Hospital/Institute
52 Fucheng Road
Haidian District
Beijing 100142
P.R. China

E-mail: youyonglu@hsc.pku.edu.cn

Date of first submission to ARS Central, September 21, 2014; date of final revised submission, January 12, 2016; date of acceptance, January 20, 2016.

Abbreviations Used

5-AZ = 5-Aza-2′-deoxycytidine
a-CAPS3 = active caspase-3
C/EBPα = CCAAT/enhancer-binding protein α
CCNB1 = cyclin B1
CCND1 = cyclin D1
ChIP = chromatin immunoprecipitation
CI = confidence interval
DATS = diallyl trisulfide
DATS+DOC = combination of diallyl trisulfide with docetaxel
DOC = docetaxel
EMSA = electrophoretic mobility shift assay
GC = gastric cancer
GI = gastrointestinal
GSK-3 = glycogen synthase kinase 3
H3K9ac = histone 3 acetylation at lysine 9
HCC = hepatocellular carcinoma
HDAC = histone deacetylase
i.p. = intraperitoneal injection
IHC = immunohistochemistry
MRE = metal responsive element
MT1A = metallothionein 1A
MT1B = metallothionein 1B
MT1E = metallothionein 1E
MT1F = metallothionein 1F
MT1G = metallothionein 1G
MT1H = metallothionein 1H
MT1M = metallothionein 1M
MT2A = metallothionein 2A
MT2A-BGC823 = GC cell line BGC823 with ectopic expression of MT2A
$MT2A^{High}$ = high MT2A expression
$MT2A^{Low}$ = low MT2A expression
MTF-1 = metal transcription factor-1
MTKO = MT1 and 2 double knockout
MTs = metallothioneins
MTT = 3-(4,5-dimethylthiazol-2-yl)-2,5-diphenyltetrazolium bromide
NF-κB = nuclear factor-kappaB
NRS = nitrogen reactive species
PD = progressive disease
p-IκB-α = phosphorylation of IκB-α
PR = partial response
ROS = reactive oxygen species
RT-PCR = reverse transcription–polymerase chain reaction
SD = stable disease
shRNA = short hairpin RNA
TNF-α = tumor necrosis factor-alpha
TSA = trichostatin A
TSA = trichostatin A
TSS = transcription start site
XIAP = X-linked inhibitor of apoptosis protein